Supplementary Information

The mechanisms of flavonoids inhibiting conformational transition of amyloid-β_{42} monomer: A comparative molecular dynamics simulation study

Ling Wang,*[abd] Ranran Zeng,[a] Xiaoqian Pang,[a] Qiong Gu*[c] and Wen Tan*[abd]

[a]Guangdong Provincial Key Laboratory of Fermentation and Enzyme Engineering, School of Bioscience and Bioengineering, South China University of Technology, Guangzhou 510006, China

[b]Pre-Incubator for Innovative Drugs & Medicine, School of Bioscience and Bioengineering, South China University of Technology, Guangzhou 510006, China

[c]Research Center for Drug Discovery, School of Pharmaceutical Sciences, Sun Yat-Sen University, Guangzhou 510006, China

[d]Key Laboratory of Industrial Biotechnology of Guangdong Higher Education Institutes, School of Bioscience and Bioengineering, South China University of Technology, Guangzhou 510006, China

*Correspondence to: lingwang@scut.edu.cn (L. Wang); guqiong@mail.sysu.edu.cn (Q. Gu); went@scut.edu.cn (W. Tan)

Contents

line), and TF (reseda line) during 20 ns MD simulation. All RMSD values were calculated with respect to the central representation structure based on clustering results from each long time comparable simulation.

Table S1. The detailed information for each simulation

Table S2. Clustering Results: Total Number of Clusters at 2.5 Å RMSD Cutoff for Each System and Number of Clusters Representing 90% of the Ensemble

Table S3. Values of the root weighted mean square inner product (RWSIP) (described in Materials and Methods) calculated by comparing the essential subspaces of pairs of simulations

Table S4. The statistical the secondary structure components of AP-Aβ_{42} and TF-Aβ_{42} with different initial velocity

Comparable simulations study for AP- and TF-A$\boldsymbol{\beta}_{42}$

Binding free energy calculation

References

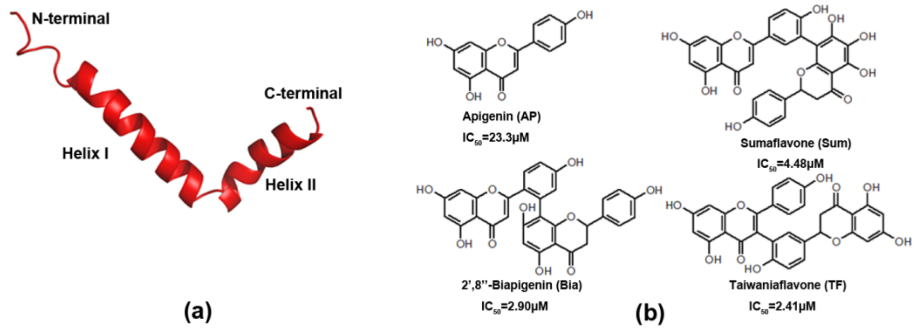

Fig. S1. The initial structure of Aβ_{42} (a) and the chemical structures of monoflavonoids (AP) and biflavonoids (Sum, Bia, and TF) (b).

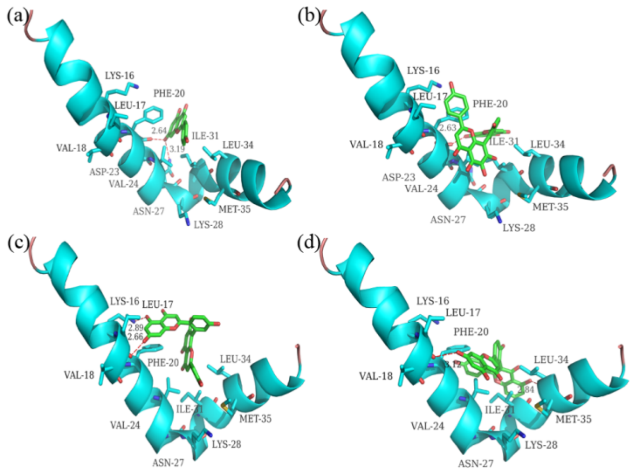

Fig. S2. The binding sites of Apigenin, Sumaflavone, 2',8''-Biapigenin, and Taiwaniaflavone (AP, Sum, Bia, and TF) on the Aβ_{42} peptide, as determined from docking calculations. The hydrogen bonds are shown with red lines.

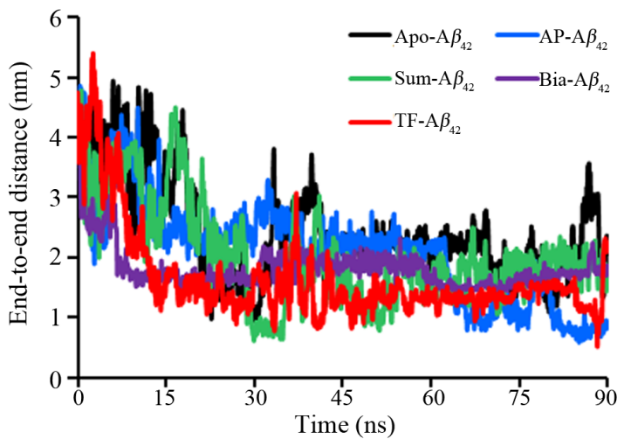

Fig. S3. End-to-end distance (the distance between Asp1-C_α and Ala42-C_α) as a function of time in all the simulations.

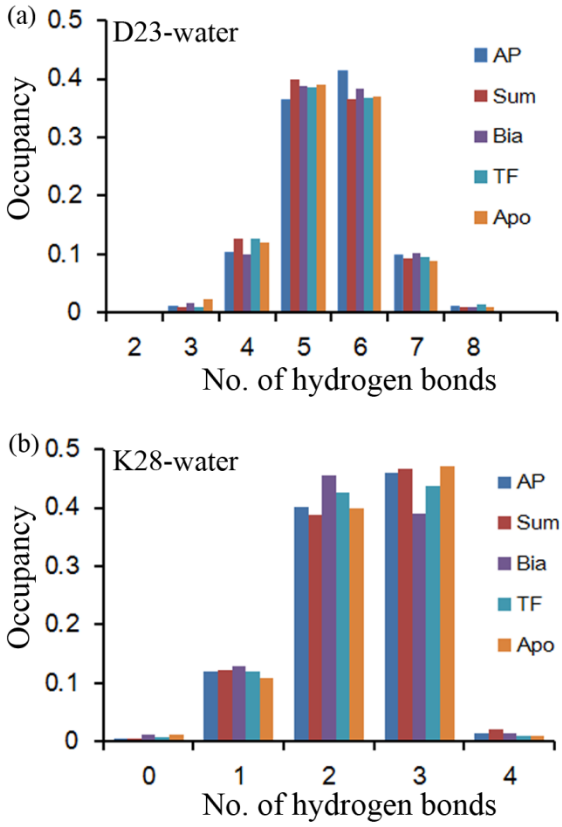

Fig. S4. The distributions of the hydrogen bonds confirm that the D23 and K28 residues were highly solvated during the MD simulations.

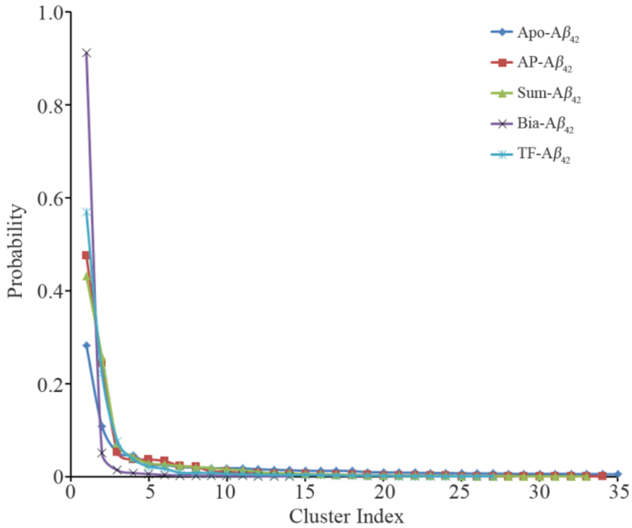

Fig. S5. The relative population distributions of the conformation clusters derived from the conformations of apo-Aβ_{42} and flavonoid-Aβ_{42} complexes. The conformations are sampled at 300 K in the MD simulations.

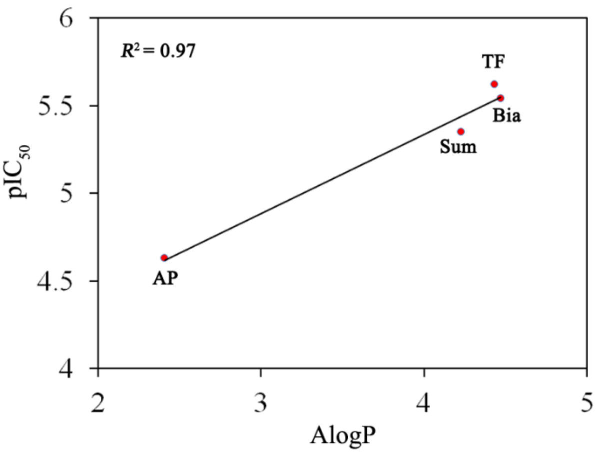

Fig. S6. The relationship of mono- and biflavonoids of inhibition activity and AlogP value. pIC50 is equal with LogIC_{50}. AlogP values of AP, Sum, Bia, and TF were calculated by Discovery studio 2.5.

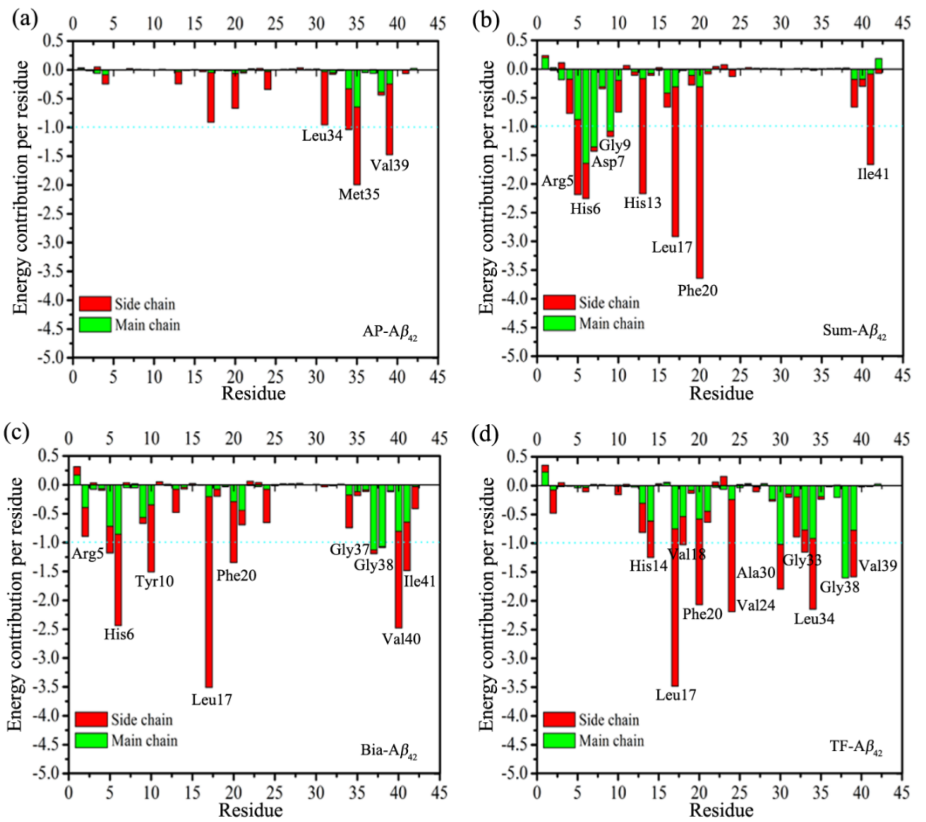

Fig. S7. Decomposition of binding free energy on contributions of main chain and side chain basis for each protein-inhibitor complex. The key residues are labeled. The unit of the each residue's contribution to total binding energy is kcal/mol.

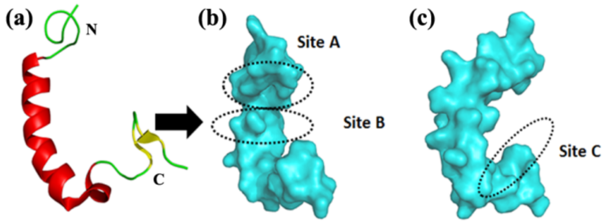

Fig. S8. (a) Conformational transition intermediate structure of Aβ_{42} from apo- Aβ_{42} simulation. (b) and (c) the surface of transition state of Aβ_{42}. A Potential drug binding pocket consists of three parts labeled by the dotted line of oval, namely Site A, Site B, and Site C, respectively. The β-sheet region at the C-terminus is the binding site.

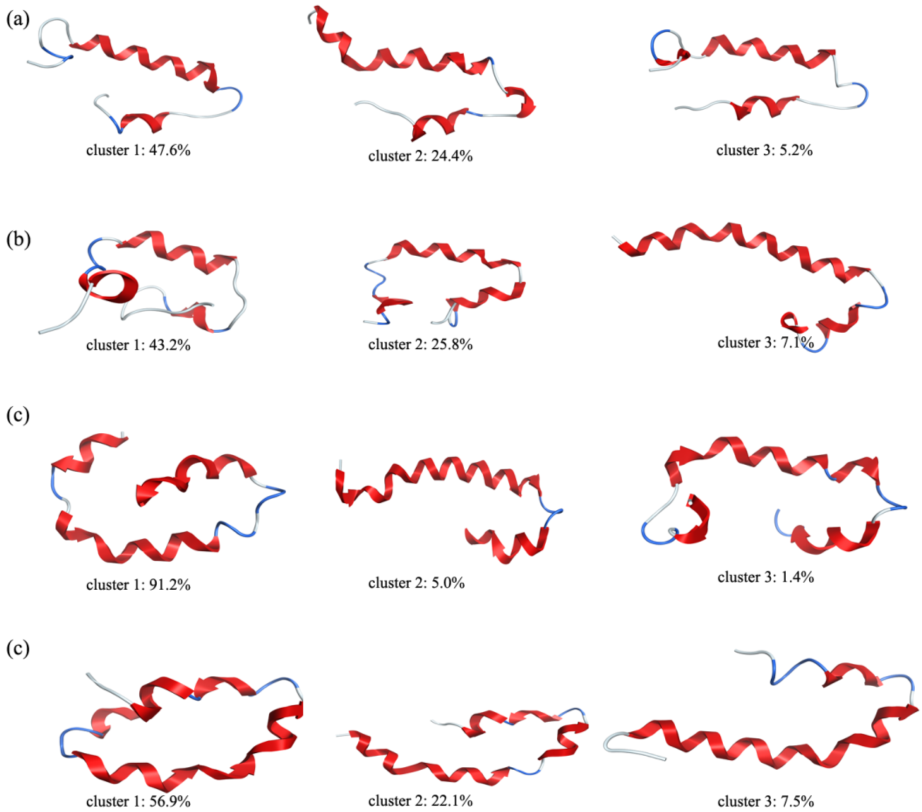

Fig. S9. A similar U-shaped state Aβ_{42} of AP-Aβ_{42} of (a), Sum-Aβ_{42} of (b), Bia-Aβ_{42} of (c), and TF-Aβ_{42} of (d) were collected from clustering results.

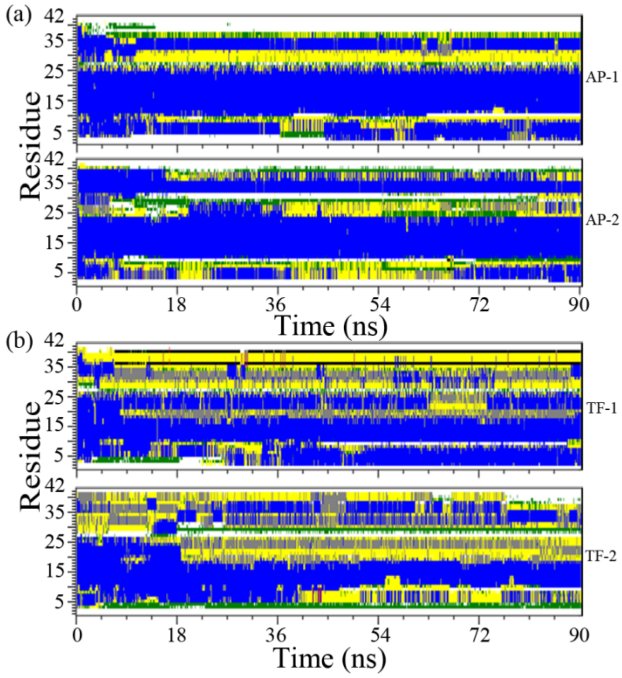

Fig. S10. Evolution of the secondary structures of (a) AP-Aβ_{42} and (b) TF-Aβ_{42} based on different initial velocity simulations.

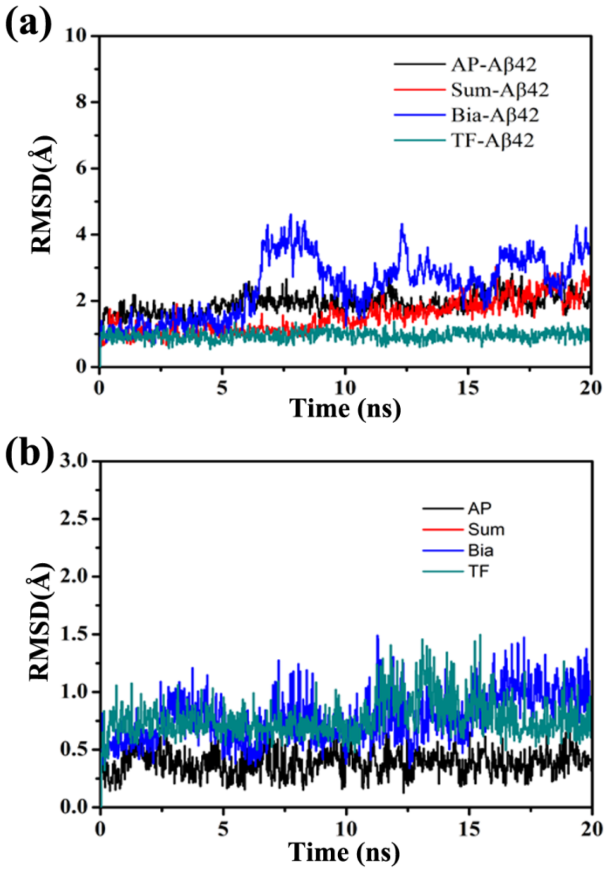

Fig. S11. (a) Time dependence of RMSD of C_α of AP-Aβ_{42} (black line), Sum-Aβ_{42} (red line), Bia-Aβ_{42} (blue line), and TF-Aβ_{42} (reseda line) during 20 ns MD simulation. (b) Time dependence of RMSD of ligand of AP (black line), Sum (red line), Bia (blue line), and TF (reseda line) during 20 ns MD simulation. All RMSD values were calculated with respect to the central representation structure based on clustering results from each long time comparable simulation.

Table S1. The detailed information for each simulation.

Model	Temperature, K	Times, ns	MMPBSA/GBSA simulations[a], ns
Apo-Aβ_{42}	300	90	–
AP-Aβ_{42}	300	90×2[b]	20
Sum-Aβ_{42}	300	90	20
Bia-Aβ_{42}	300	90	20
TF-Aβ_{42}	300	90×2[b]	20

[a]The additional simulations for mono- and biflavonoids-Aβ_{42} complex to calculate binding free energies. [b] two dependent simulations with different initial velocity to test our simulations are reliable and repeatable rather than a stochastic output (due to the machine, force filed and parameter file).

Table S2. Clustering results: total number of clusters at 2.5 Å RMSD cutoff for each system and number of clusters representing 90% of the ensemble.

system	cluster1	cluster2	cluster3	cluster4	cluster5	total no. of clusters	90% ensemble
Apo	28.3	10.9	5.2	4.5	2.6	158	53
AP	47.6	24.4	5.2	3.7	3.7	35	7
Sum	43.2	25.8	7.1	4.2	2.8	33	8
Bia	91.2	5.0	1.4	0.7	0.5	14	1
TF	56.9	22.1	7.5	3.7	2.1	27	4

Table S3. Values of the root weighted mean square inner product (RWSIP) (described in Materials and Methods) calculated by comparing the essential subspaces of pairs of simulations.

RMSIP	Apo	AP	Sum	Bia
AP	0.712	-	-	-
Sum	0.714	0.763	-	-
Bia	0.739	0.693	0.689	-
TF	0.670	0.753	0.729	0.773

Table S4. The statistical the secondary structure components of AP-Aβ_{42} and TF-Aβ_{42} with different initial velocity.

Secondary structure	AP-1	AP-2	TF-1	TF-2
coil	18.19	17.81	10.97	14.26
β-sheet	0.00	0.00	0.00	0.00
β-bridge	0.00	0.05	4.21	0.00
turn	17.82	8.71	24.29	22.78
bend	5.16	14.30	3.14	7.91
helix	58.83	59.12	57.39	55.05

Comparable simulations study for AP-Aβ_{42} and TF-Aβ_{42}. To make certain that our simulations are repeatable rather than a stochastic output (due to the machine, force filed and parameter file), two independent simulations with different initial velocity distributions are performed for AP-Aβ_{42} and TF-Aβ_{42}. Conformational transition of Aβ_{42} is a key index for testing the reliable and repeatable of Aβ_{42} simulation. For two different initial velocity simulations, conformational transition and secondary structure components of Aβ_{42} were calculated and compared as follows. As shown in Figure S2, two dependent simulations exhibited similar conformational transition. The detailed secondary structure components of Aβ_{42} are listed in Table S3. From this table, major components of helix and coil structures are very similar, only different for linker structure (e.g. bend or turn), similarity results can be found in other publications [1-4]. In short, our simulations are reliable and repeatable rather than a stochastic output (due to the machine, force filed and parameter file).

Binding free energy calculation. We simulate each model for an additional 20 ns in order to calculate the binding free energies for mono- and biflavonoids-Aβ_{42} complex and to provide insight into interaction energy and energetic stability of mono- and biflavonoids-Aβ_{42} complex. The initial each complex coordinate was the central representation structure based on clustering results from each long time comparable simulation. The force field parameters of protein and ligand were applied for AMBER ff03 force field and Generalized Amber force field (GAFF), respectively. The simulations are done with the AMBER 12. For mono- and biflavonoids-Aβ_{42} system, free energy calculations was performed on 1000 snapshot structures extracted at 10 ps intervals over the last 10 ns stable MD trajectory (Figure S6). For each snapshot structure, the binding free energy was calculated for both enzyme-inhibitor complexes through the molecular mechanics Poisson-Boltzmann surface area (MM-PBSA) and generalized Born (MM-GBSA) methods [5, 6]. In the MM-PBSA and MM-GBSA approach an interaction free energy is defined as

$$\Delta G_{binding} = G_{complex} - [G_{protein} + G_{ligand}] \quad (1)$$

Where $G_{complex}$, $G_{protein}$, and G_{ligand} are the free energies of the complex, protein and the ligand, respectively. Each free energy term in eq 1 was computed as sum of the absolute free energy in the gas phase (E_{gas}), the solvation free energy ($G_{solvation}$), and the entropy term (TS), using eq 2:

$$G = E_{gas} + G_{solvation} - TS \quad (2)$$

E_{gas} was expressed as the sum of changes in the van der Waals energy (E_{vdw}), electrostatic energy (E_{ele}), and the internal energies (E_{int}) in the gas phase (eq 3). E_{int} is the energy associated with vibration of covalent bonds and bond angels, rotation of single bond torsional angels (eq 4)

$$E_{gas} = E_{int} + E_{vdw} + E_{ele} \quad (3)$$

$$E_{int} = E_{bond} + G_{angel} + E_{torsion} \quad (4)$$

The solvation free energy, $G_{solvation}$, is approximated as the sum of the polar contribution ($G_{PB/GB}$) and nonpolar contribution ($G_{nonpolar}$) using continuum solvent methods:

$$G_{solvation} = G_{PB/GB} + G_{nonpolar} \quad (5)$$

$$G_{nonpolar} = \gamma \times SASA + b \quad (6)$$

The polar contribution ($G_{PB/GB}$) to the solvation energy was calculated either using the PB and GB model implemented in AMBER 12. The grid size used is 0.5 Å. The dielectric constant was set to 1 for interior solute and 80 for exterior water. The nonpolar contributions ($G_{nonpolar}$) were estimated using eq 6, where SASA is the solvent-accessible surface area that was estimated using the linear combination of pairwise overlaps (LCPO) [7]; the probe radius of 1.4 Å, γ = 0.0072 kcal·mol^{-1}·Å^{-2}, and b=0 kcal/mol (eq 6).

The calculation of the entropic contribution is computationally expensive and omitted in our study because it requires extremely well minimized structures for a normal-mode analysis or large numbers of snapshots for a quasi-harmonic analysis [8]. Furthermore, the binding free energy decomposition was performed on a per-residue basis using the molecular mechanics generalized Born/surface area (MM-GBSA) method [9-11]. This decomposition was carried out only for molecular mechanics and solvation energies but not for entropies.

References

1. R. Kayed, E. Head, J. L. Thompson, T. M. McIntire, S. C. Milton, C. W. Cotman and C. G. Glabe, *Science*, 2003, **300**, 486-489.
2. J. Hardy and D. J. Selkoe, *Science*, 2002, **297**, 353-356.
3. C. Yang, X. Zhu, J. Li and R. Shi, *J. Mol. Model.*, 2010, **16**, 813-821.
4. Y. C. Xu, J. J. Shen, X. M. Luo, W. L. Zhu, K. X. Chen, J. P. Ma and H. L. Jiang, *Proc. Natl. Acad. Sci. U.S.A.*, 2005, **102**, 5403-5407.
5. P. A. Kollman, I. Massova, C. Reyes, B. Kuhn, S. H. Huo, L. Chong, M. Lee, T. Lee, Y. Duan, W. Wang, O. Donini, P. Cieplak, J. Srinivasan, D. A. Case and T. E. Cheatham, *Accounts Chem. Res.*, 2000, 33, 889-897.
6. J. M. J. Swanson, R. H. Henchman and J. A. McCammon, *Biophys. J.*, 2004, 86, 67-74.
7. J. Weiser, P. S. Shenkin and W. C. Still, *J. Comput. Chem.*, 1999, **20**, 217-230.
8. M. A. S. Perez, S. F. Sousa, E. F. T. Oliveira, P. A. Fernandes and M. J. Ramos, *J. Phys. Chem. B.*, 2011, **115**, 15339-15354.
9. V. Tsui and D. A. Case, *Biopolymers*, 2000, **56**, 275-291.
10. G. Rastelli, A. Del Rio, G. Degliesposti and M. Sgobba, *J. Comput. Chem.*, 2010, **31**, 797-810.
11. V. Zoete, M. B. Irving and O. Michielin, *J. Mol. Recognit.*, 2010, **23**, 142-152.